

Theoretical study of magnetism in transition-metal-doped TiO_2 and $\text{TiO}_{2-\delta}$

L. A. Errico and M. Rentería

Departamento de Física, Instituto de Física La Plata (CONICET), Facultad de Ciencias Exactas, Universidad Nacional de La Plata,
C.C. No. 67, 1900 La Plata, Argentina

M. Weissmann

Departamento de Física, Comisión Nacional de Energía Atómica, Avenida del Libertador 8250, 1429 Buenos Aires, Argentina

(Received 23 August 2005; published 22 November 2005)

In recent years there has been an intense search for room temperature ferromagnetism in semiconductors doped with dilute magnetic impurities, in particular, oxides. In this work we study the structural, electronic, and magnetic properties of doped rutile TiO_2 for two different impurity concentrations (25% and 6.25%), considering different distributions of the impurities in the host lattice. Calculations were performed with *ab initio* methods, assuming that the magnetic impurities substitutionally replace the Ti ions. Our results show that a local magnetic moment appears in the cases of Mn, Fe, and Co impurities, but not in the cases of Ni and Cu impurities. They also show that in the system $\text{Ti}_{1-x}\text{Co}_x\text{O}_2$ the magnetic ions align ferromagnetically, while in $\text{Ti}_{1-x}\text{Mn}_x\text{O}_2$ and $\text{Ti}_{1-x}\text{Fe}_x\text{O}_2$ the antiferromagnetic alignment is energetically favorable. We have also studied the effect of oxygen vacancies, which turned out to be very important. Their presence decreases the energy required to introduce the impurities in the host lattice and reciprocally, the presence of impurities is related to a higher vacancy concentration. The pairs impurity-nearest-neighbor oxygen vacancy seem to be the energetically preferred structures and to produce the highest local magnetic moments. Ni and even Cu impurities acquire magnetic moments in this environment.

DOI: [10.1103/PhysRevB.72.184425](https://doi.org/10.1103/PhysRevB.72.184425)

PACS number(s): 75.50.Pp, 71.20.Nr, 75.50.Dd, 71.15.Mb

I. INTRODUCTION

Dilute magnetic impurities in semiconductors (DMS) produce materials that may be ferromagnetic at room temperature and are therefore appealing for spintronics (see, e.g., Refs. 1–3 and references therein). This is a rapidly developing research area because the electron spin may play a separate role, in addition to the usual charge degree of freedom. DMS's based on II-VI compound semiconductors such as Mn-doped CdTe and ZnSe (Ref. 4) were the first to be studied. However, this family of DMS's has a Curie temperature (T_C) in the order of 1 K and is therefore not useful for practical applications. DMS's based on III-V semiconductor compounds, such as Mn-doped GaAs (Ref. 5), have T_C as high as 110 K but this is still far from room temperature. Research efforts continued in order to find higher T_C 's and recently room-temperature ferromagnetism has been observed in other Mn-doped compounds, such as CdGeP₂,⁶ ZnGeP₂,⁷ and ZnO.⁸ In 2001, Matsumoto *et al.*⁹ reported that Co-doped anatase TiO_2 films grown by a combinatorial pulsed-laser-deposition (PLD) molecular beam epitaxy (MBE) technique can keep ferromagnetic order up to 400 K. The measured saturated magnetic moment per Co atom was $0.32\mu_B/\text{Co}$ for Co concentration up to 8%. More recently, Co-doped anatase TiO_2 films grown by the oxygen-plasma-assisted (OPA) MBE were reported by Chambers *et al.*¹⁰ to have a magnetic moment of $1.26\mu_B/\text{Co}$. It is interesting to note that Matsumoto *et al.* observed magnetic behavior in Co-doped TiO_2 anatase, but not in the rutile phase, suggesting that the magnetization of the Co atoms could depend on the local structure around it. However, in 2002, Park *et al.* were able to grow ferromagnetic Co-doped TiO_2 rutile films

by sputtering and T_C was also estimated to be above 400 K.¹¹ The measured magnetic moment was $0.94\mu_B/\text{Co}$ and the Co concentration 12%. This variety of results motivated intensive experimental^{12,13} and theoretical^{14–19} studies of the structural, magnetic, and electronic properties of doped TiO_2 . Since the rutile structure is thermodynamically more stable than the anatase one, it could have a higher potential for technical applications if thin films could be grown easily.

The microscopic mechanism of long-range magnetic order is still an open problem. Carrier-induced interaction between the magnetic atoms was suggested as the reason for ferromagnetism in III-V based DMS.²⁰ However, subsequent reports raised concerns about this idea, due to the possibility of ferromagnetic metal clustering under different growth conditions.^{8,21} Furthermore, it has been suggested that the strong interaction between Co and oxygen vacancies in Co-doped TiO_2 plays a key role for the explanation of its high T_C .^{14,17,22,23} Experimental results also suggest that oxygen defects may be responsible for the observed ferromagnetism in Fe-doped TiO_2 samples.²⁴ The location and distribution of the impurities in the host lattices is still unclear; while Soo *et al.*¹³ found through extended x-ray absorption fine structure spectroscopy (EXAFS) that the local environment surrounding Co impurities remains anatase-like, Kim *et al.*²⁵ and Shinde *et al.*²⁶ claim that Co tends to cluster and form metallic Co.

As most previous theoretical and experimental studies for doped rutile TiO_2 have considered only Co and Fe impurities, we have extended the study to other transition metal dopants. We present here a set of density-functional-theory-based calculations in the systems $\text{Ti}_{1-x}\text{R}_x\text{O}_2$ ($R=\text{Mn, Fe, Co, Ni, Cu}$) for different impurity concentrations and distributions. Calculations were performed with the full-potential

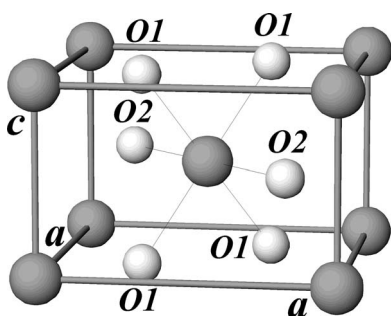


FIG. 1. Unit cell of rutile TiO_2 (Ti gray balls, O: white balls).

linearized-augmented plane waves (FLAPW) method and with the SIESTA code assuming that the magnetic impurities substitutionally replace the Ti atoms. The case of impurity-atom clusters was not considered, as an exhaustive investigation of the energetics of impurity complexes in TiO_2 is outside the scope of the present work.

A local magnetic moment appeared in Mn, Fe, and Co doped systems and the consideration of different distributions of the impurities in the host allowed us to evaluate the exchange coupling parameters (J_{ij}) that give the tendency to ferromagnetism or antiferromagnetism. Calculations for oxygen-deficient systems showed that impurities with nearest-neighbor oxygen vacancies are the energetically more favorable structures and those with the largest magnetic moments.

The paper is organized as follows: in Sec. II we report the structures studied and computational details; in Sec. III we discuss the electronic and magnetic properties of the Mn, Fe, Co, Ni, and Cu impurities in rutile TiO_2 as a function of the impurity concentration; in Sec. IV we discuss the magnetic ordering for different impurity distributions; in Sec. V we discuss the effect of oxygen vacancies in the structural and magnetic properties of the systems $\text{Ti}_{1-x}\text{R}_x\text{O}_2$. Finally, in Sec. VI we present our conclusions.

II. THE SYSTEM UNDER STUDY AND COMPUTATIONAL DETAILS

TiO_2 has three possible structures: rutile, anatase, and brookite, rutile being the most stable. For our calculations we chose the first one, because fewer theoretical studies of TiO_2 doped with magnetic impurities were performed for that case. There is an additional advantage of the rutile structure: a small supercell can be used for the simulations and a quite uniform distribution of defects is obtained, which is not the case for anatase. It therefore leads to a more realistic approximation of the structural distortions induced by the impurity and the vacancies in the host lattice. The unit cell of rutile TiO_2 is tetragonal ($a=b=4.5845_1 \text{ \AA}$, $c=2.953_2 \text{ \AA}$,²⁷ space group $P42/mnm$) (see Fig. 1) and contains two metal atoms (Ti) at positions $(0, 0, 0)$ and $(1/2, 1/2, 1/2)$ and four oxygen atoms (O) at positions $(u, u, 0)$; $(1/2+u, 1/2-u, 1/2)$ with $u=0.30493_7$.²⁷ The structure has only one crystallographic Ti site. These Ti atoms are surrounded by a slightly distorted octahedron of oxygen atoms, with a rectangular

basal plane (O1) at a distance of 1.94 \AA from Ti and two vertex atoms (O2) at 1.98 \AA . In the case of O, there is only one crystallographic site, and each oxygen atom is surrounded by three Ti. All the calculations were performed for the bulk material as the experimental thin films are thick enough to contain many unit cells.

The spin-polarized electronic-structure calculations presented in this work were performed with the FLAPW method²⁸ as embodied in the WIEN97 code,²⁹ in a scalar relativistic version without spin-orbit coupling. Exchange and correlation effects were treated within density-functional theory using both the local spin density³⁰ (LSDA) and the generalized gradient³¹ (GGA) approximations. The atomic spheres radii (muffin tins), R_i , used for Ti and O were 1.01 and 0.85 \AA , respectively, while for the magnetic impurities we used $R_i=1.06 \text{ \AA}$. The parameter $RK_{MAX}=R_{mt} * K_{MAX}$, which controls the size of the basis set in these calculations, was chosen as eight for the smallest supercell employed and seven for the largest ones (R_{mt} is the smallest muffin tin radius and K_{MAX} the largest wave number of the basis set). We introduced local orbitals to include Ti- $3s$ and $3p$, O- $2s$ and Mn-, Fe-, Co-, Ni-, and Cu- $3p$ orbitals. The number of k points was increased until convergence was reached. In order to study the relaxation introduced by the impurities we computed the forces on the atoms³² and moved them until the forces on the ions were below a tolerance value. Because the volume change associated with substitutional (and even interstitial) $3d$ transition metal impurities has only a negligible effect on the formation heat of $\text{Ti}_{1-x}\text{R}_x\text{O}_2$,¹⁶ we fixed the lattice parameters at the experimentally determined bulk TiO_2 values and optimized only internal parameters upon doping.

We also employed, especially for structural minimizations, the SIESTA code,³³ which uses a linear combination of numerical real-space atomic orbitals as basis set and norm-conserving pseudopotentials.³⁴ We proved in selected systems that the relaxed structures predicted by SIESTA are in agreement with those predicted by WIEN97. In all the cases we also proved using WIEN97 that the relaxed structures predicted by SIESTA have lower energies than the unrelaxed ones and that both methods give similar magnetic moments.

III. STUDY OF THE SYSTEMS $\text{Ti}_{1-x}\text{R}_x\text{O}_2$

We studied the systems $\text{Ti}_{1-x}\text{R}_x\text{O}_2$ ($R=\text{Mn, Fe, Co, Ni, Cu}$) for two impurity concentrations ($x=0.0625$ and 0.25) with the WIEN97 code. The supercell (SC) considered consisted of two unit cells of TiO_2 stacked along the c axis with one Ti atom replaced by the magnetic impurity [Fig. 2(a)]. The resulting 12-atoms SC (Ti_3RO_8 in the following) has dimensions $a'=b'=a$, $c'=2c$. The impurity concentration in this SC is 25% ($x=0.25$). The second SC employed consisted of eight units cells of TiO_2 [Fig. 2(b)], corresponding to an impurity concentration of 6.25% ($x=0.0625$). The resulting 48-atoms SC ($\text{Ti}_{15}\text{RO}_{32}$) has dimensions $a'=b'=2a$, $c'=2c$.

As the results obtained with the LSDA and GGA approximations are very similar, for the sake of simplicity we will present here only those obtained using the LSDA approximation. We found that the presence of magnetic impurities in-

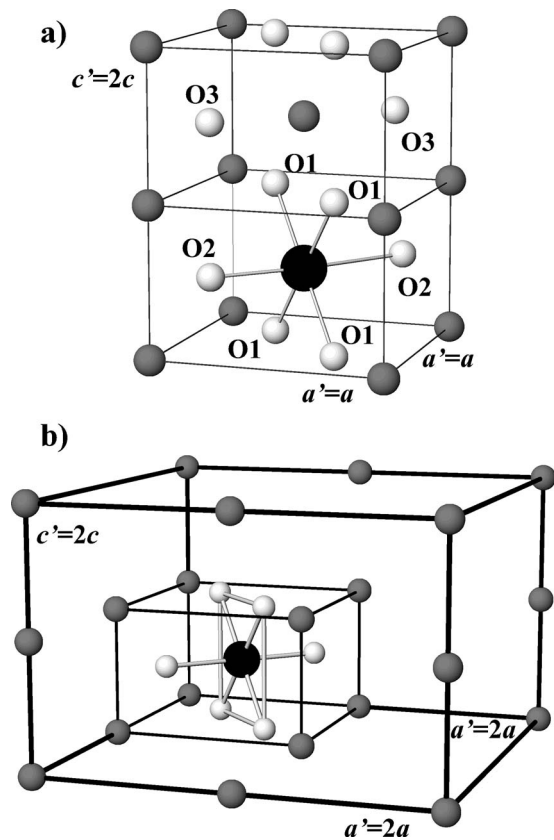


FIG. 2. Supercells used in the calculations for the two impurity concentrations studied (Ti, gray balls, O, white balls; impurity black balls). (a) 12-atoms SC (Ti_3RO_8); (b) 48-atoms SC ($\text{Ti}_{15}\text{RO}_{32}$). Not all O and Ti atoms are shown for clearness.

duces local geometrical distortions (contractions) in the first oxygen neighbors (ONN) of the impurities. The bond lengths R -O1 and R -O2 are reduced about 0.05 \AA in the case of Ti_3RO_8 (see Table I). These structural distortions are nearly isotropic and their magnitudes are small and essentially independent of the impurity considered. This can be related to the similar ionic radii of the impurities and the Ti atoms. Similar structural distortions were found in the case of $\text{Ti}_{15}\text{RO}_{32}$, the differences in the magnitude of the contractions being smaller than 0.02 \AA . In the case of Cu the structural distortions induced by the impurity are anisotropic, the

TABLE I. Relaxed bond lengths d between the impurity R and the two types of neighbor oxygen atoms in rutile TiO_2 (O1 and O2) for an impurity concentration of 25% (Ti_3RO_8) and magnetic moments in the muffin tin sphere of the impurities (μ^{imp}) and in the supercell (μ^{SC}).

System	$d(R\text{-O1})$	$d(R\text{-O2})$	μ^{imp}	μ^{SC}
TiO_2	1.94 \AA	1.98 \AA	$0.00\mu_B$	$0.00\mu_B$
Ti_3MnO_8	1.91 \AA	1.95 \AA	$2.52\mu_B$	$3.04\mu_B$
Ti_3FeO_8	1.89 \AA	1.96 \AA	$2.24\mu_B$	$2.58\mu_B$
Ti_3CoO_8	1.90 \AA	1.93 \AA	$0.63\mu_B$	$1.03\mu_B$
Ti_3NiO_8	1.91 \AA	1.95 \AA	$0.00\mu_B$	$0.00\mu_B$
Ti_3CuO_8	1.93 \AA	2.02 \AA	$0.00\mu_B$	$0.00\mu_B$

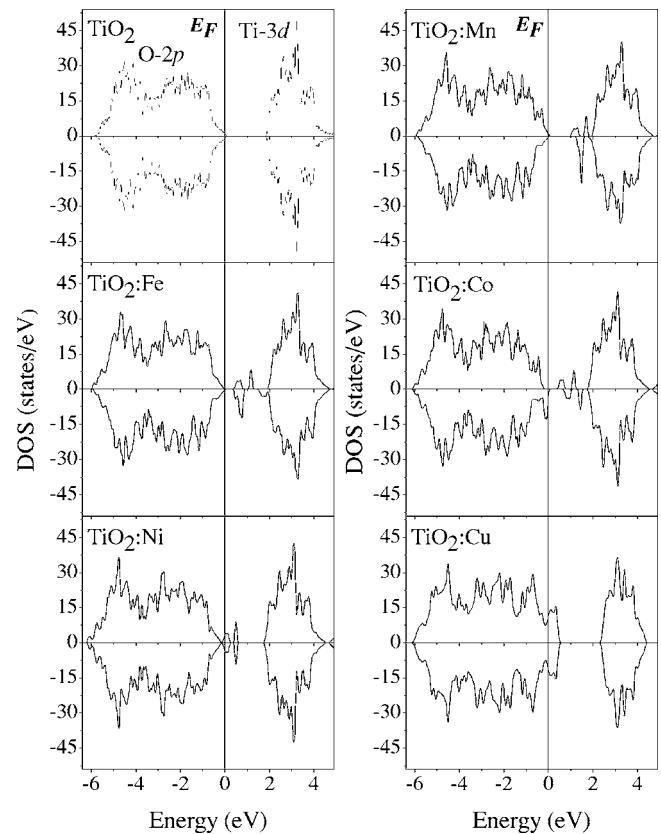


FIG. 3. Calculated total density of states (DOS) of the systems $\text{Ti}_{15}\text{R}_x\text{O}_{32}$ ($R=\text{Ti, Mn, Fe, Co, Ni, Cu}$). Energies are referred to the Fermi level (E_F).

Cu-O1 bond lengths are shorter while the Cu-O2 distances are enlarged by about 0.04 \AA (see Table I).

Regarding electronic and magnetic properties, we found that the magnetic moments in $\text{Ti}_{1-x}\text{Mn}_x\text{O}_2$ and $\text{Ti}_{1-x}\text{Fe}_x\text{O}_2$ are larger than that of $\text{Ti}_{1-x}\text{Co}_x\text{O}_2$, and that $\text{Ti}_{1-x}\text{Ni}_x\text{O}_2$ is not magnetic. As it was expected, no magnetic moment was found in the case of $\text{Ti}_{1-x}\text{Cu}_x\text{O}_2$. In Table I we present the obtained magnetic moments in the atomic spheres of the impurities and in the whole SC for all the impurities considered. Spin-polarization occurs mainly at the impurity sites, but the nearest-neighbor oxygens can be polarized up to $0.06\mu_B/\text{ONN}$. The magnetic moments are almost independent of the impurity concentration and of the structural distortion. The results obtained for the cases of Co and Mn agree qualitatively with those obtained theoretically by Yang *et al.*¹⁵ for Co in anatase TiO_2 and Park *et al.* for Mn in the same host.¹⁴ However, Park *et al.* also performed calculations for Fe in anatase TiO_2 and obtained a magnetic moment of $3.7\mu_B$ for the system $\text{Ti}_{15}\text{FeO}_{32}$, larger than that for $\text{Ti}_{15}\text{MnO}_{32}$ ($3.0\mu_B$), in contradiction with the trend we show in Table I.

In Fig. 3 we show the density of states (DOS) for pure and doped rutile TiO_2 obtained by FLAPW calculations for the systems $\text{Ti}_{15}\text{RO}_{32}$. The overall band structure of TiO_2 is consistent with previous works (see, for example, Ref. 35), the band gap is smaller than the experimental value^{9,36} due to the well-known problem of band gap underestimation in the LDA approximation. While for this concentration the sys-

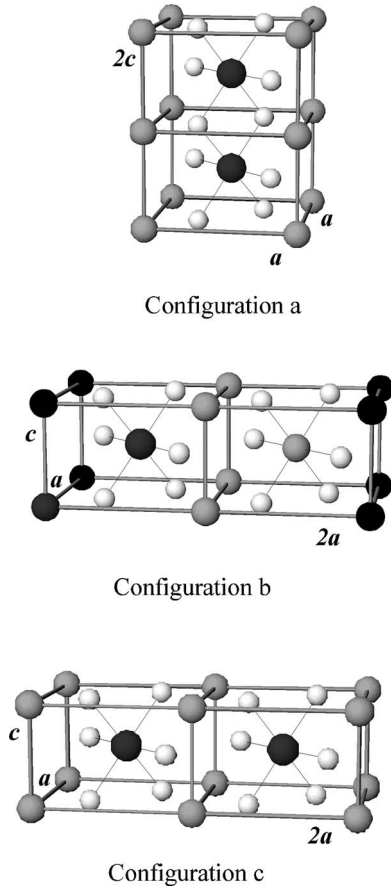


FIG. 4. 12-atoms supercells with two impurity atoms (black balls) in three different distributions within the TiO_2 host.

tems doped with Mn, Fe, and Co show a reduced band gap, those doped with Ni and Cu are metallic. For the larger concentration (smaller SC) the features inside the gap increase in size and the systems doped with Co also become metallic. From the partial DOS projected in the different muffin-tin spheres we find that the states inside the gap have, apart from the d -character due to the impurities, contributions from the neighboring O1- and O2- p states, that increase with Z or the number of d electrons.

IV. MAGNETIC ORDERING

In the previous paragraph ferromagnetic alignment was assumed for the calculations, as only one impurity per unit cell was considered. To be able to determine if the impurities tend to align ferromagnetically (FM) or antiferromagnetically (AF), we performed calculations with two impurities in the unit cell, for three different impurity distributions, considering parallel and antiparallel spins. Figure 4 shows the three supercells used. The first one (Fig. 4, configuration *a*) consists of two unit cells of TiO_2 stacked along the c axis with the two central Ti atoms replaced by the magnetic impurities. The second and third SCs also consist of two unit cells of TiO_2 , but stacked along the a axis. In Fig. 4 configuration *b*, one impurity replaces a Ti ion located at the corner of a cell and the other replaces the Ti ion located at the center of the same cell. In Fig. 4 configuration *c*, the central Ti in the two cells are replaced by the magnetic impurities. Table II shows the energies for the FM and AF cases and the local magnetic moment of each configuration. Within a simple Ising model, the total energy difference between the FM and AF alignments (Δ_{AF}) can be related to the exchange coupling constants J_{ij} among impurities at sites i and j and to the Curie temperature. The total energy of a system in a specific magnetic state can be approximated as

$$E = - \sum_{j,i} J_{ij} S_i S_j, \quad (1)$$

where S_i and S_j represent the spins of the impurities at sites i and j (we take $|S|=5/2, 2,$ and $3/2$ for Mn, Fe, and Co, respectively) and the sum runs over all the impurities up to a certain neighboring shell. Knowing the total energy differences $E_{AF} - E_F = \Delta_{AF}$ for different impurity distributions it is possible to estimate some of the exchange parameters. The number of J_{ij} 's that one can estimate depends on the number of different magnetic structures that can be stabilized in the self-consistent calculations, while limiting the unit cell to a reasonable size.

For simplicity we shall drop an index on the J_{ij} coefficients and refer to $J_{1,2,3}$ as the coupling constant among first, second, and third neighbor impurities. Also, we find it more convenient to describe the results of Table II not following

TABLE II. Calculated total energies, referred to the nonmagnetic case, exchange coupling constants J_i , and local magnetic moments μ for Mn, Fe, and Co in rutile TiO_2 for the different configurations studied (see Fig. 4).

Impurity	Configuration	E_F (eV)	E_{AF} (eV)	J_i (10^{-3} eV)	μ_F (μ_B)	μ_{AF} (μ_B)
Mn	<i>a</i>	-2.00	-2.06		2.66	2.57
	<i>b</i>	-1.63	-1.73	$J_1 = +2.1; J_2 = +2.0; J_3 = +1.6$	2.66	2.58
	<i>c</i>	-2.01	-2.05		2.66	2.64
Fe	<i>a</i>	-0.56	-0.80		1.74	2.20
	<i>b</i>	-0.30	-0.46	$J_1 = +14.3; J_2 = +4.9; J_3 = -2.2$	2.67	1.88
	<i>c</i>	-0.57	-0.53		1.81	1.68
Co	<i>a</i>	-0.04	-0.001		0.60	0.16
	<i>b</i>	-0.16	-0.10	$J_1 = -4.4; J_2 = -3.3; J_3 = -2.1$	0.61	0.52
	<i>c</i>	-0.04	-0.003		0.58	0.57

TABLE III. Distance (in Å) from the vacancy site to its cations nearest neighbors in the relaxed structures of Ti_3RO_7 . The first row corresponds to oxygen-deficient TiO_2 . In square brackets we indicate the multiplicity. We also indicate the nature of the neighbor, when it is not Ti.

$TiO_{2-\delta}$	2.34/2.17 [2] Vacancy at O1	Vacancy at O2	Vacancy at O3
Ti_3MnO_7	1.96 (Mn)/2.20/2.30	2.12 (Mn)/2.12 [2]	2.13 [2]/2.31
Ti_3FeO_7	2.06 (Fe)/2.23/2.33	2.14 (Fe)/2.21 [2]	2.15 [2]/2.32
Ti_3CoO_7	2.04 (Co)/2.24/2.33	2.13 (Co)/2.11 [2]	2.14 [2]/2.32
Ti_3NiO_7	2.01 (Ni)/2.25/2.31	1.95 (Ni)/2.08 [2]	2.12 [2]/2.30
Ti_3CuO_7	2.00 (Cu)/2.22/2.33	2.07 (Cu)/2.12 [2]	2.13 [2]/2.30

the order of the Periodic Table. In the case of Co impurities the most stable structures are those ferromagnetically aligned; the magnetic moments are independent of the impurity distribution and very similar to those obtained in Sec. III. In the case of Mn impurities the local magnetic moments are independent of the concentration, of the configuration, and of the magnetic ordering considered, and they are four times larger than those for $Ti_{1-x}Co_xO_2$. The most stable phases in this case are antiferromagnetically aligned, as one would expect for Mn. In the case of Fe impurities, we find that the magnetic moment depends on the configuration considered, and also that for some configurations the most stable phase is antiferromagnetic. For this impurity, the possibility of obtaining a stable ferromagnetic semiconductor with a large magnetic moment, depends on the distribution of the impurities in the TiO_2 lattice and, as we shall see in the Sec. V, on the number and distribution of oxygen vacancies.²⁴ Since for Fe and Mn impurities the AF alignment is favored, we should expect, within a mean-field picture, a rather small Curie temperature.

V. THE ROLE OF OXYGEN VACANCIES

The origin of ferromagnetism and high Curie temperature (T_C) of rutile and anatase $Ti_{1-x}Co_xO_{2-\delta}$ and $Ti_{1-x}Fe_xO_{2-\delta}$ is still controversial. The experimental results depend strongly on the growth conditions of the samples.^{9,10,23,24} For example, samples produced in oxygen-rich atmospheres show negligible magnetization;³⁷ and Kim *et al.*²⁵ and Shinde and Ogale²⁶ found that Co clusters were present in their samples. On the other hand, the experimental results obtained by Suryanarayanan *et al.* in Fe- and Co-doped TiO_2 films point out the important role played by the oxygen vacancies in the ferromagnetic properties of Fe/Co substituted TiO_2 films.^{23,24}

From the theoretical point of view, the interaction of magnetic ions and oxygen vacancies has been discussed in a few papers and the results are controversial. In Refs. 14 and 17 first-principles calculations were performed to study the role of oxygen vacancies on the magnetic properties of Co-doped TiO_2 . Park *et al.*¹⁴ showed that the oxygen vacancy near a Ti site is more stable than near Co and that in such situation the magnetic moment is $2.53\mu_B$. Weng *et al.*¹⁷ obtained from their calculations that the oxygen vacancy prefers to stay near the Co impurity, and that the magnetic moment is

$0.90\mu_B$. Other papers assume strong electron-electron correlations and use different approximate methods so that their results are not comparable to the present calculations.²²

In order to analyze the effect of oxygen vacancies in the doped systems we first studied the undoped one, $TiO_{2-\delta}$ with $\delta=0.08$. For this calculation we used a SC similar to Fig. 2(a), but without the impurity and removing an oxygen atom (Ti_4O_7) and took into account the structural distortions produced by the vacancy. Although the volume change associated with a large concentration of vacancies may be important, we decided to keep the lattice parameters fixed so as to make all the results comparable. The structural distortions are much larger than those found for the systems Ti_3RO_8 and $Ti_{15}RO_{32}$: some of the Ti atoms are displaced as much as 0.3 Å away from the vacancy location (see Table III). Concerning the electronic properties, the Fermi level moves into the conduction band, making the system metallic. When a spin polarized calculation was performed for this system we found that there were two possible degenerate solutions, one nonmagnetic and the other having a magnetic moment of approximately $1\mu_B$ per SC, due to polarization of the Ti atoms. It is worth mentioning that the magnetic phase appeared only when the structural relaxation was taken into account. This unexpected result anticipated that a large concentration of oxygen vacancies could play an important role in the magnetic behavior of doped rutile TiO_2 . To check this we performed calculations with a larger unit cell and only one vacancy ($Ti_{16}O_{31}$), both in rutile and anatase structures. We obtained a smaller magnetic moment for the rutile structure and none for the anatase structure. It seems that the appearance of a magnetic moment may depend on the vacancy concentration in the oxide and on the structure. An experimental observation of magnetism in an undoped nonmagnetic oxide has been recently reported and attributed to vacancies also.³⁸

Next, we studied the oxygen deficient systems Ti_3RO_7 , considering the three possibilities for removing an oxygen atom from the SC: (i) from the Ti-contained octahedron [O3 in Fig. 2(a)], (ii) from the impurity-contained octahedron removing a basal O atom (O1), and (iii) from the impurity-contained octahedron removing a vertex O atom (O2). In all cases, we found that the structural relaxations induced by the oxygen vacancy are larger than those produced by the impurity (see Tables I and IV). We also found that the cations that are nearest neighbors to the vacancy site are repelled from it

TABLE IV. Distance (in Å) of the impurity R to its oxygen nearest neighbors in the relaxed structures of Ti_3RO_7 . The number in brackets indicates the multiplicity.

	Vacancy at O1	Vacancy at O2	Vacancy at O3
Ti_3MnO_7	1.92/2.02 [2]/2.00	1.95 [4]/2.07	1.94/2.09 [4]
Ti_3FeO_7	1.90/1.95 [2]/1.98	1.93 [4]/2.01	1.92/2.00 [4]
Ti_3CoO_7	1.85/1.94 [2]/1.97	1.94 [4]/2.01	1.93/2.00 [4]
Ti_3NiO_7	1.86/1.96 [2]/1.99	1.92 [4]/2.07	1.97/2.08 [4]
Ti_3CuO_7	1.81/2.05 [2]/2.00	2.15 [4]/2.00	2.00/2.10 [4]

(Table III). Comparing the total energies of the three cases we found that the oxygen vacancies near the impurities are more stable than those near Ti for all the cases studied [Fig. 5(a)], in agreement with the result found by Weng *et al.*¹⁷ for Co in oxygen-deficient TiO_2 . In Fig. 5(a) we can also see that the energy required to form an oxygen vacancy decreases from approximately 10 eV in the undoped system to much smaller values in the doped ones. This effect is more important if the vacancies are close to the impurities and if the number of d electrons increases. Also, the energy required to substitute a Ti atom by an impurity is strongly reduced when there is an oxygen vacancy in the SC. This reduction is larger for Cu and for nearest-neighbor impurity-vacancy pairs [see Fig. 5(b)]. We therefore predict that doped systems will have more vacancies than undoped ones, and that oxygen vacancies will tend to be close to the impurities. We also calculated the system with two oxygen vacancies in the SC and found that the energy required to form two vacancies near an impurity is larger than that necessary to create one vacancy in the first shell of neighbors of two differ-

ent impurities. For this reason, we discard the existence of vacancy clusters around the impurity atoms. However, in case each impurity had already one vacancy close to it a new vacancy would prefer to go there and not to be isolated.

Concerning the magnetic properties of the systems Ti_3RO_7 , we found that the magnetic solutions have lower energy than the nonmagnetic ones, the magnetic moment being due mostly to polarization of the impurity atoms. Table V shows that the presence of a vacancy close to the impurity (in O1) increases the magnetic moment of the unit cell when there already was magnetic moment and induces a magnetic moment for Ni and Cu. These results support the idea that ferromagnetism strongly depends on the oxygen deficiency, and the different magnetic moments observed in samples grown by different methods and/or different conditions can thus be understood. The nonmagnetic impurity (Cu) was included in these studies because unexpected ferromagnetism was observed experimentally in TiO_2 films doped with Cu.³⁹ It is interesting to note that covalency is larger in bonds between Cu and its ONN, and for this reason the magnetic moment is not so localized in this case. In view of this, it seems now questionable to describe the new type of magnetism with a Heisenberg model Hamiltonian, and also to estimate Curie temperatures with it.

Figure 6 shows the DOS for pure and doped rutile TiO_2 with one oxygen vacancy in O1 in the 12-atom SC. The main effect of the vacancy is to move the Fermi level towards the conduction band, so that many of the impurity states inside the gap are occupied and the systems become metallic.

As these calculations were performed using a small SC, with one impurity and one vacancy in it, there is a large and equal concentration of both. To make contact with experimental results one should be able to use a larger SC and average over different concentrations and distributions of im-

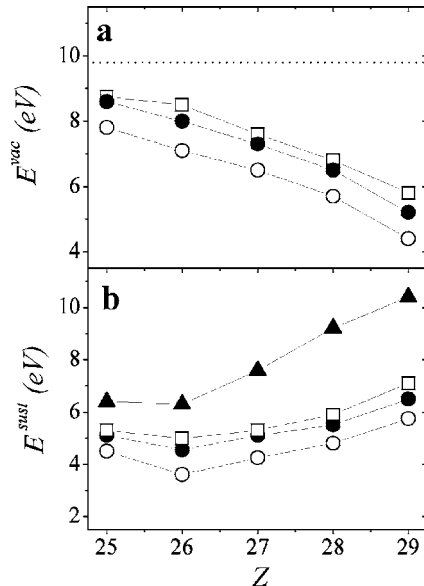


FIG. 5. Vacancy formation energies (a) and substitution energies in the presence of vacancies; (b) for the different impurities, represented by their atomic number Z . Open circles: vacancy at O1; solid circles: vacancy at O2; open squares vacancy at O3. Dotted line in (a) is the energy necessary to generate an oxygen vacancy in pure TiO_2 . Solid triangles in (b) are the substitution energies in stoichiometric TiO_2 . Solid lines are just to guide the eyes.

TABLE V. Magnetic moments in the muffin tin spheres of the impurities (μ^{imp}) and in the SC (μ^{SC}) for the different impurities and vacancy positions in the relaxed structures.

	Vacancy at O1 $\mu^{\text{imp}} / \mu^{\text{SC}}$	Vacancy at O2 $\mu^{\text{imp}} / \mu^{\text{SC}}$	Vacancy at O3 $\mu^{\text{imp}} / \mu^{\text{SC}}$
Ti_3MnO_7	3.73/4.98	3.23/3.65	3.78/5.02
Ti_3FeO_7	3.20/4.00	2.06/2.21	2.13/2.51
Ti_3CoO_7	0.81/1.02	0.87/0.99	0.40/0.70
Ti_3NiO_7	1.08/1.50	0.00/0.00	1.42/1.97
Ti_3CuO_7	0.56/1.01	0.55/1.01	0.57/0.99

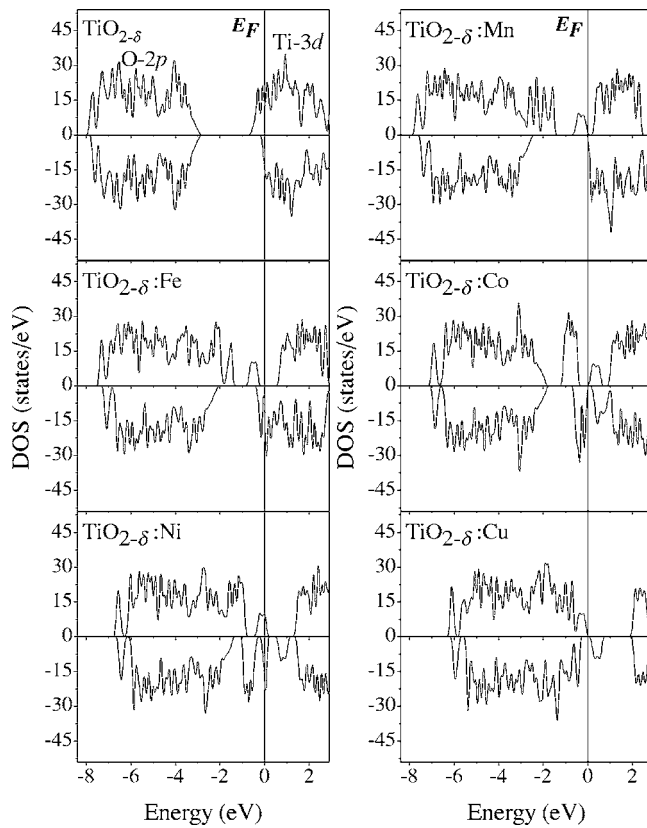


FIG. 6. Calculated total DOS of the oxygen-deficient (Ti_3RO_7) systems. Energies are referred to the Fermi level (E_F).

purities and vacancies, which seems a formidable task. We have performed, however, a few calculations with the 48-atom SC and confirmed that the previous results are all qualitatively correct. We therefore believe that oxygen vacancies in the adequate proportion can provide the necessary carriers to account for ferromagnetic behavior.

VI. CONCLUSIONS

We have presented here an *ab initio* study of the systems $\text{Ti}_{1-x}\text{R}_x\text{O}_2$ ($R=\text{Mn, Fe, Co, Ni, Cu}$) for different substitu-

tional impurity concentrations, in the rutile structure. We found that magnetic moments appear for Mn, Fe, and Co, but not for Ni and Cu. They are originated on the impurity d states, which are hybridized with p -oxygen states, and a related feature appears in the host band energy gap. The values of these magnetic moments are almost independent of the impurity concentration when no oxygen vacancies are considered. The magnetic ordering results antiferromagnetic for Mn and also for Fe in some geometrical distributions but ferromagnetic for Co. Using a simple Ising model we calculated the exchange coupling parameters J_{ij} for first, second, and third neighbors and their relative values for the different impurities could be compared in the future with experimental data.

When oxygen vacancies are introduced along with the magnetic impurities our results show that the energetically preferred vacancy location is that of nearest neighbor to the impurity. Additionally, we found that the strong interaction between oxygen vacancies and impurities increases the local magnetic moment in the cases of Mn, Fe, and Co and induces a magnetic behavior in the cases of Ni and Cu. An important result of these calculations is that doping lowers the formation energy of vacancies, so that doped systems will have more vacancies than the undoped ones. These results support the hypothesis that oxygen vacancies play an important role in the origin of magnetism in doped TiO_2 , and can explain the diversity of magnetic moments observed experimentally for samples grown in different conditions.

ACKNOWLEDGMENTS

This work was partially supported by Agencia Nacional de Promoción Científica y Tecnológica (ANPCyT), PICT98 03-03727, Consejo Nacional de Investigaciones Científicas y Técnicas (CONICET), PEI6174 and PIP6032, Fund. Antorchas, Argentina, and the Third World Academy of Sciences (TWAS), Italy, RGA 97-057. We thank R. Weht for his assistance with the SIESTA code and to C. E. Rodríguez Torres, and A. F. Cabrera for helpful discussions.

¹H. Ohno, Science **281**, 951 (1998).

²T. Dietl, H. Ohno, F. Matsukura, J. Cibert, and D. Ferrand, Science **287**, 1019 (2000).

³T. Fukumura, Y. Yamada, H. Toyosaki, T. Hasegawa, H. Koinuma, and M. Kawasaki, Appl. Surf. Sci. **223**, 62 (2004).

⁴J. K. Furdyna and J. Kossut, *DMSs, Semiconductors and Semimetals* (Academic Press, New York, 1988), Vol. 25.

⁵H. Ohno, A. Shen, F. Matsukura, A. Oiwa, A. Endo, S. Katsumoto, and Y. Iye, Appl. Phys. Lett. **69**, 363 (1996).

⁶G. A. Medvedkin, T. Ishibashi, T. Nishi, K. Hayata, Y. Hasegawa, and K. Sato, Jpn. J. Appl. Phys., Part 2 **39**, L949 (2000).

⁷S. Cho, S. Choi, G. B. Cha, S. C. Hong, Y. Kim, Y. J. Zhao, A. J. Freeman, J. B. Ketterson, B. J. Kim, Y. C. Kim, and B. C. Choi, Phys. Rev. Lett. **88**, 257203 (2002).

⁸P. Sharma, A. Gupta, K. V. Rao, F. J. Owens, R. Sharma, R. Ahuja, J. M. Osorio Guillen, B. Johansson, and G. A. Gehring, Nat. Mater. **24**, 673 (2003).

⁹Y. Matsumoto, M. Murakami, T. Shono, T. Hasegawa, T. Fukumura, M. Kawasaki, P. Ahmet, T. Chikyow, S. Koshihara, and H. Koinuma, Science **291**, 854 (2001).

¹⁰S. A. Chambers, S. Thevuthasan, R. F. C. Farrows, R. F. Marks, J. U. Thiele, L. Folks, M. G. Samant, A. J. Kellock, N. Ruzycski, D. L. Ederer, and U. Diebold, Appl. Phys. Lett. **79**, 3467 (2001); S. A. Chambers, Mater. Today **5**, 34 (2002).

¹¹W. K. Park, R. J. Ortega-Hertogs, J. S. Moodera, A. Punnoose, and M. S. Seehra, Appl. Phys. Lett. **91**, 8093 (2002).

¹²W. Prellier, A. Fouchet, and B. Mercey, J. Phys.: Condens. Matter **15**, R1583 (2003).

- ¹³Y. L. Soo, G. Kioseoglou, S. Kim, Y. H. Kao, P. Sujatha, J. Parise, R. J. Gambino, and P. I. Gouma, *Appl. Phys. Lett.* **81**, 655 (2002).
- ¹⁴M. S. Park, S. K. Kwon, and B. I. Min, *Phys. Rev. B* **65**, 161201(R) (2002).
- ¹⁵Z. Yang, G. Liu, and R. Wu, *Phys. Rev. B* **67**, 060402(R) (2003).
- ¹⁶W. T. Geng and K. S. Kim, *Phys. Rev. B* **68**, 125203 (2003).
- ¹⁷H. Weng, X. Yang, J. Dong, H. Mizuseki, M. Kawasaki, and Y. Kawasoe, *Phys. Rev. B* **69**, 125219 (2004).
- ¹⁸L. A. Errico, M. Weissmann, and M. Rentería, *Phys. Status Solidi B* **241**, 2399 (2004).
- ¹⁹L. A. Errico, M. Weissmann, and M. Rentería, *Physica B* **354**, 338 (2004).
- ²⁰H. Munekata, H. Ohno, S. von Molnar, A. Segmüller, L. L. Chang, and L. Esaki, *Phys. Rev. Lett.* **63**, 1849 (1989).
- ²¹S. R. Shinde, S. B. Ogale, S. Das Sarma, J. R. Simpson, H. D. Drew, S. E. Lofland, C. Lanci, J. P. Buban, N. D. Browning, V. N. Kulkarni, J. Higgins, R. P. Sharma, R. L. Greene, and T. Venkatesan, *Phys. Rev. B* **67**, 115211 (2003).
- ²²V. I. Anisimov, M. A. Korotin, L. A. Nekrasov, A. S. Mylnikova, J. L. Wang, and Z. Zeng, cond-mat/0503625 (unpublished).
- ²³R. Suryanarayanan, V. M. Naik, P. Kharel, P. Talagala, and R. Naik, *Solid State Commun.* **133**, 439 (2005).
- ²⁴R. Suryanarayanan, V. M. Naik, P. Kharel, P. Talagala, and R. Naik, *J. Phys.: Condens. Matter* **17**, 755 (2005).
- ²⁵J. Y. Kim, J. H. Park, B. G. Park, H. J. Noh, S. J. Oh, J. S. Yang, D. H. Kim, S. D. Bu, T. W. Noh, H. J. Lin, H. H. Hsieh, and C. T. Chen, *Phys. Rev. Lett.* **90**, 017401 (2003).
- ²⁶S. R. Shinde and S. B. Ogale, cond-mat/0203576 (unpublished).
- ²⁷J. Hill and C. J. Howard, *J. Appl. Crystallogr.* **20**, 467 (1987).
- ²⁸S. H. Wei and H. Krakauer, *Phys. Rev. Lett.* **55**, 1200 (1985).
- ²⁹P. Blaha, K. Schwarz, P. Dufek, and J. Luitz, WIEN97, Vienna University of Technology, 1997. Improved and updated Unix version of the original copyrighted Wien-code, which was published by P. Blaha, K. Schwarz, P. I. Sorantin, and S. B. Trickey, in *Comput. Phys. Commun.* **59**, 399 (1990).
- ³⁰J. P. Perdew and Y. Wang, *Phys. Rev. B* **45**, 13244 (1992).
- ³¹J. P. Perdew, K. Burke, and M. Ernzerhof, *Phys. Rev. Lett.* **77**, 3865 (1996).
- ³²R. Yu, D. Singh, and H. Krakauer, *Phys. Rev. B* **43**, 6411 (1991).
- ³³P. Ordejón, E. Artacho, and J. M. Soler, *Phys. Rev. B* **53**, R10441 (1996); D. Sánchez-Portal *et al.*, *Int. J. Quantum Chem.* **65**, 453 (1997).
- ³⁴N. Troullier and J. L. Martins, *Phys. Rev. B* **43**, 1993 (1991).
- ³⁵P. I. Sorantin and K. Schwarz, *Inorg. Chem.* **31**, 567 (1992).
- ³⁶J. Pascual, J. Camassel, and H. Mathieu, *Phys. Rev. B* **18**, 5606 (1978).
- ³⁷S. A. Chambers, S. M. Heald, and T. Droubay, *Phys. Rev. B* **67**, 100401(R) (2003).
- ³⁸M. Venkatesan, C. B. Fitzgerald, and J. M. D. Coey, *Nature (London)* **430**, 630 (2004).
- ³⁹S. Duhalde, M. F. Vignolo, F. Golmar, C. Chilotte, C. E. Rodríguez Torres, L. A. Errico, A. F. Cabrera, M. Rentería, F. H. Sánchez, and M. Weissmann, *Phys. Rev. B* **72**, 161313(R) (2005).